ISCI, Volume *22*

Supplemental Information

MTA3 Represses Cancer Stemness by Targeting the SOX2OT/SOX2 Axis

Liang Du, Lu Wang, Jinfeng Gan, Zhimeng Yao, Wan Lin, Junkuo Li, Yi Guo, Yuping Chen, Fuyou Zhou, Sai-Ching Jim Yeung, Robert P. Coppes, Dianzheng Zhang, and Hao Zhang

Supplemental figures and legends

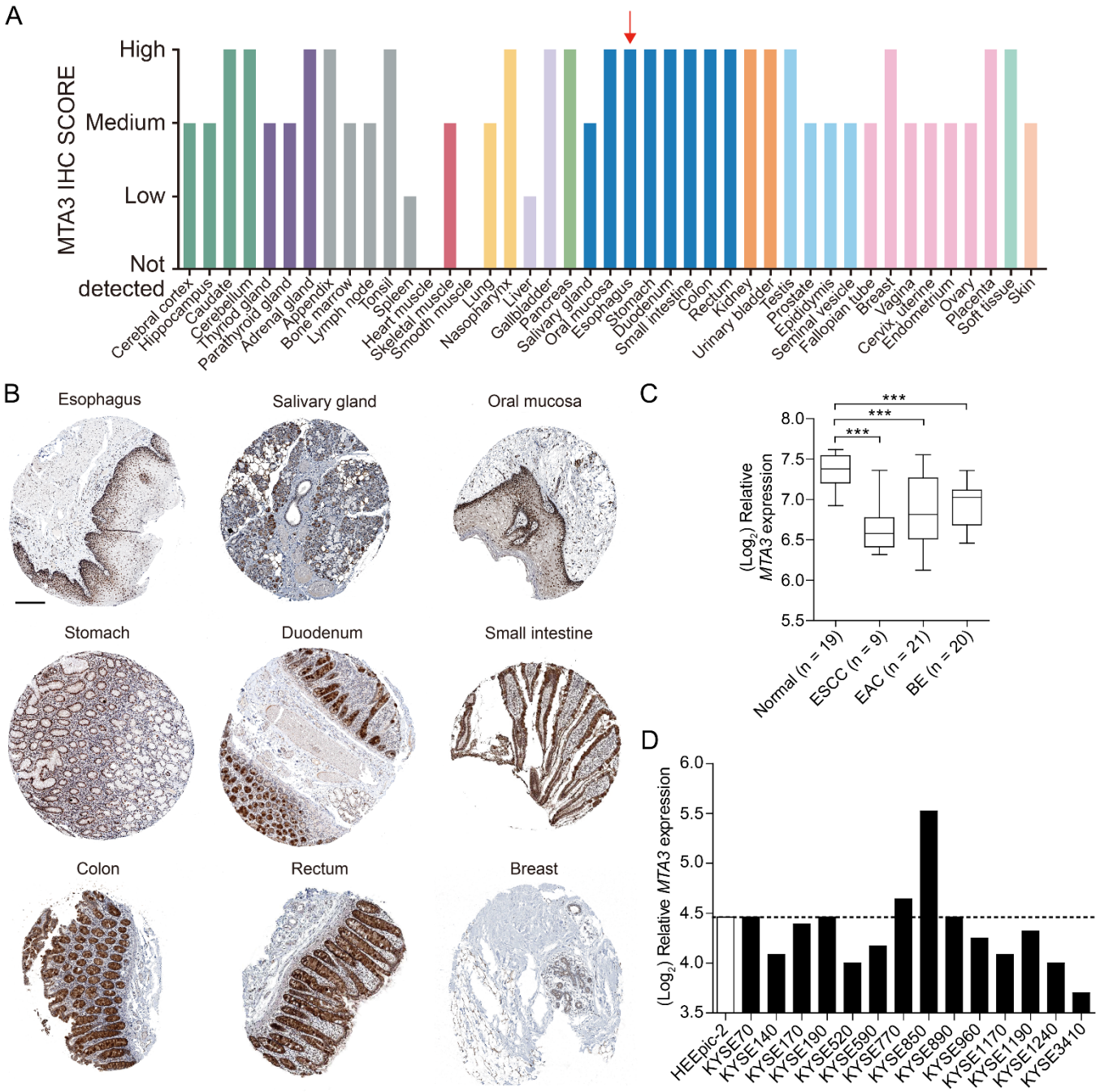

Figure S1. Related to Figure 1. MTA3 is highly enriched in human digestive organs and downregulated in human esophageal squamous cell carcinoma (ESCC). (**A**) IHC score of MTA3 in various human normal organs was investigated in the Human Protein Atlas database, red arrow indicates *esophagus*. **(B)** Representative IHC images of MTA3 in the indicated digestive organs, including esophagus, breast was used as positive control. All images were obtained from Human Protein Atlas database. Scale bars: 200 μm. (**C**) *MTA3* mRNA expression in an ESCC microarray dataset from GEO, GSE26886. (**D**)

MTA3 mRNA expression in a panel of ESCC cell lines (filled bars) and normal esophageal epithelium cells (open bar) was analyzed in a microarray dataset from GEO, GSE23964. ***$p < 0.001$ by one-way ANOVA with post hoc intergroup comparisons.

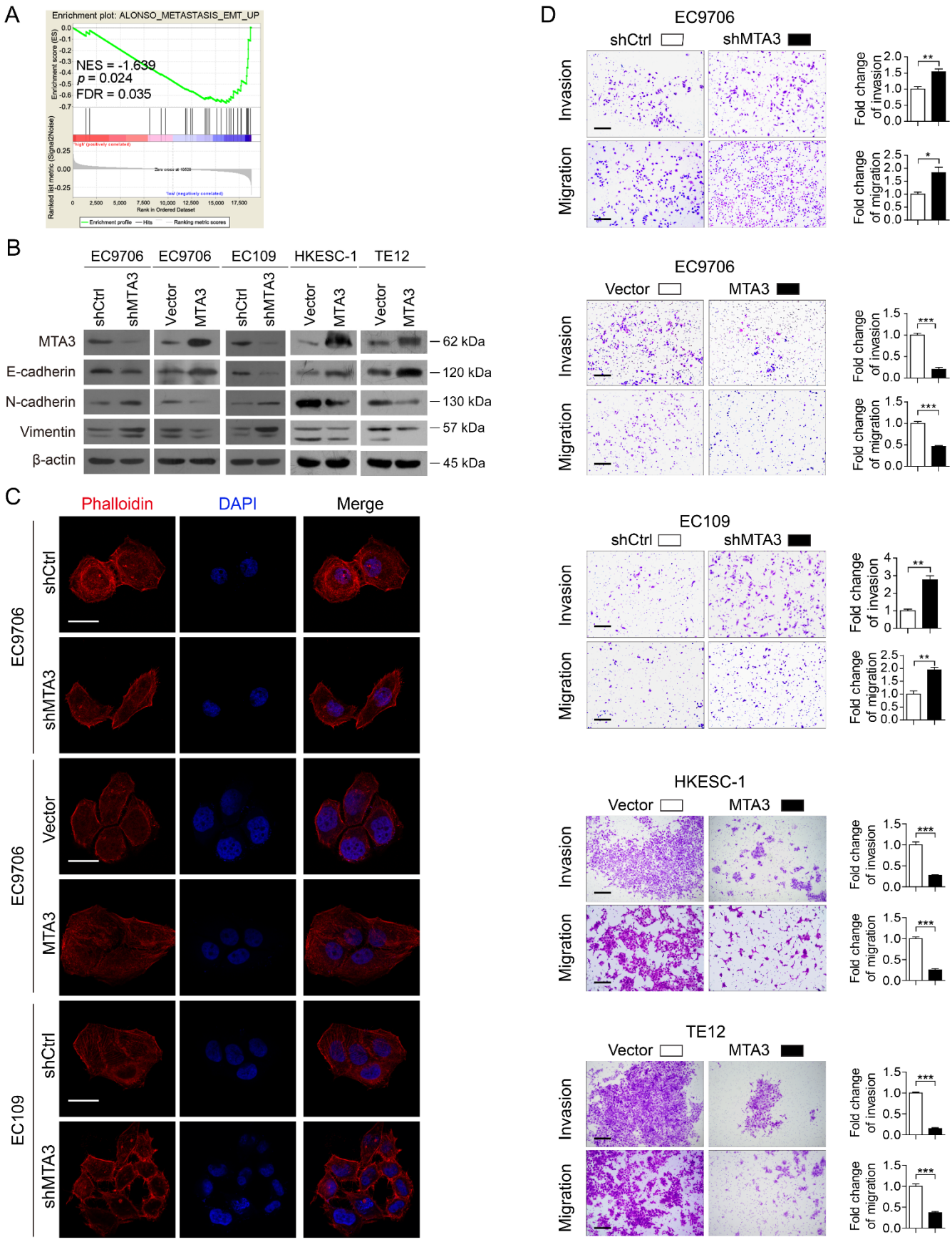

Figure S2. Related to Figure 2. MTA3 suppresses the metastatic potential of ESCC cells *in vitro*. (**A**) GSEA plots of enrichment of ALONSO_METASTASIS_EMT_UP signatures in $MTA3^{High}$ tumors versus $MTA3^{Low}$ tumors in GSE23400 dataset. (**B**) Western blot of the indicated epithelial or mesenchymal

markers and MTA3 in EC9706 cells with MTA3 depletion or overexpression, and EC109 cells with MTA3 depletion, and in HKESC-1 cells and TE12 cells with MTA3 overexpression. β-actin is shown as a loading control. (**C**) Representative images of phalloidin staining of EC9706 cells with MTA3 depletion or overexpression and EC109 cells with MTA3 depletion. Scale bars: 20 μm. (**D**) Invasion or migration of EC9706 cells with MTA3 depletion or overexpression, EC109 cells with MTA3 depletion, and HKESC-1 cells and TE12 cells with MTA3 overexpression were measured by transwell assay with or without matrigel. Scale bars: 200 μm. Data were shown as means of three independent experiments. Error bars indicate SEM. *$p< 0.05$, **$p< 0.01$, ***$p< 0.001$ by Student's *t*-test.

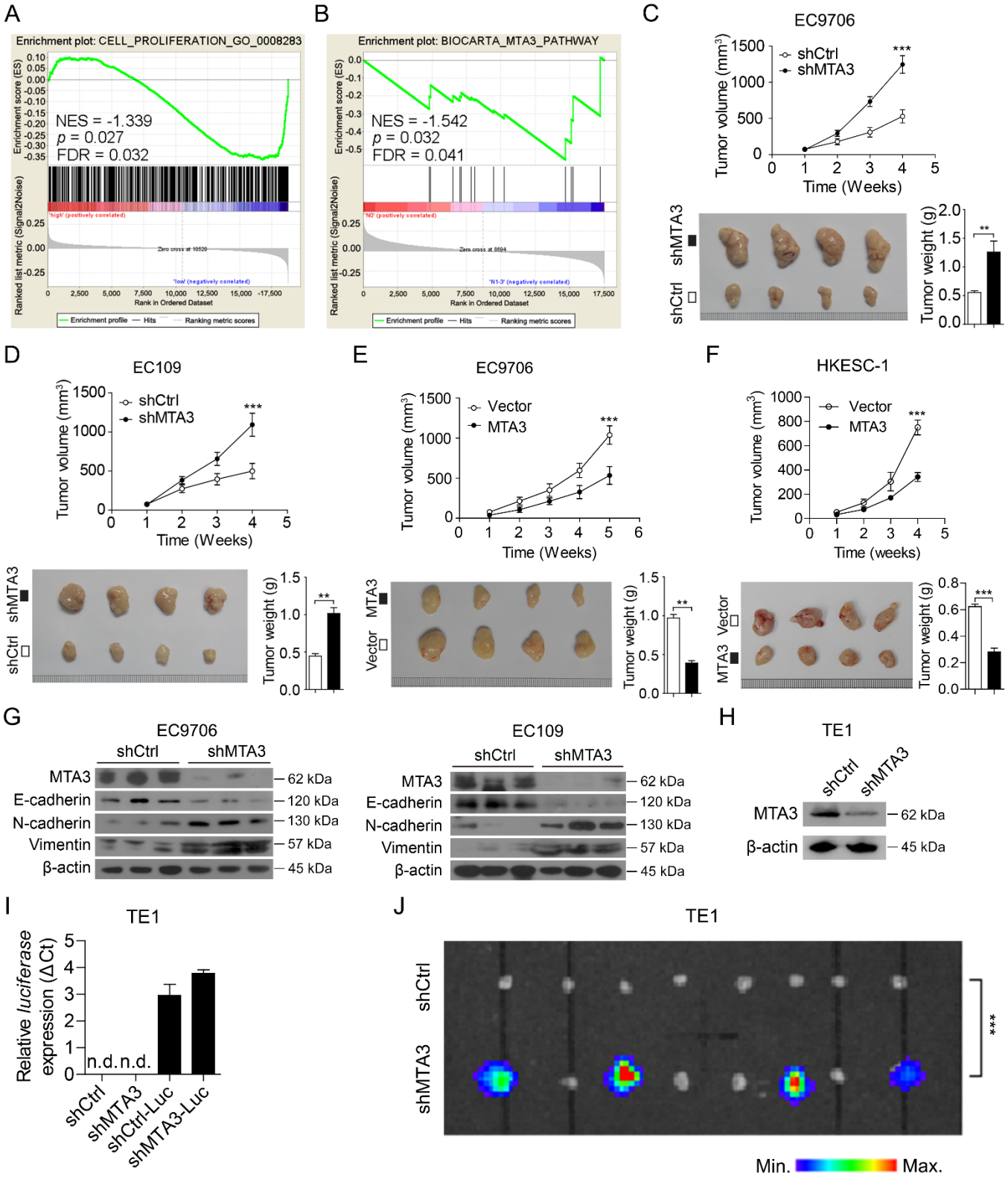

Figure S3. Related to Figure 2. MTA3 regulates the tumor growth of ESCC cells and metastasis *in vivo*. (**A**) GSEA plots of enrichment of CELL_PROLIFERATION_GO_0008283 signatures in MTA3^{High} tumors versus MTA3^{Low} tumors in the GSE23400 dataset. (**B**) GSEA plots of enrichment of BIOCARTA_MTA3_PATHWAY in ESCC tissues with non-lymph node metastasis versus ESCC tissues with lymph node metastasis in the GSE47404 dataset. (**C**) Growth curves for tumor formation of the

EC9706 cells with MTA3 depleted were generated (upper panel). Tumors were resected (lower left panel) and weighed (lower right panel) at the end of the experiments (n = 5 shCtrl, n = 5 shMTA3). (**D**) Growth curves for tumor formation of the EC109 cells MTA3 depleted were generated (upper panel). Tumors were resected (lower left panel) and weighed (lower right panel) at the end of the experiments (n = 5 shCtrl, n = 5 shMTA3). (**E**) Growth curves for tumor formation of the EC9706 cells with MTA3 overexpressed were generated (upper panel). Tumors were resected (lower left panel) and weighed (lower right panel) at the end of the experiments (n = 5 Vector, n = 5 MTA3). (**F**) Growth curves for tumor formation of the HKESC-1 cells with MTA3 overexpressed were generated (upper panel). Tumors were resected (lower left panel) and weighed (lower right panel) at the end of the experiments (n = 5 Vector, n = 5 MTA3). (**G**) Western blot of the indicated epithelial or mesenchymal markers and MTA3 in tumors derived from EC9706 cells with MTA3 depleted (left panel) and EC109 cells with MTA3 depleted (right panel). **(H)** Western blot of MTA3 in TE1 cells with MTA3 depleted. (**I**) TE1 cells that transfected with shMTA3 or shCtrl were infected with lentiviruses carrying luciferase and then subjected for RNA extraction followed by qRT-PCR analysis of luciferase gene. (**J**) The TE1 cells with or without MTA3 depleted were infected with recombinant lentiviruses carrying luciferase and injected subcutaneously into the flanks of nude mice (n = 8). The inguinal lymph nodes of the mice were extracted and analyzed for the presence of metastatic cells by bioluminescence imaging. Data were shown as the means from at least three independent experiments or representative data. Error bars indicate SEM. $^{**}p<0.01$, $^{***}p<0.001$ by Student's *t*-test or chi-square test, where appropriate.

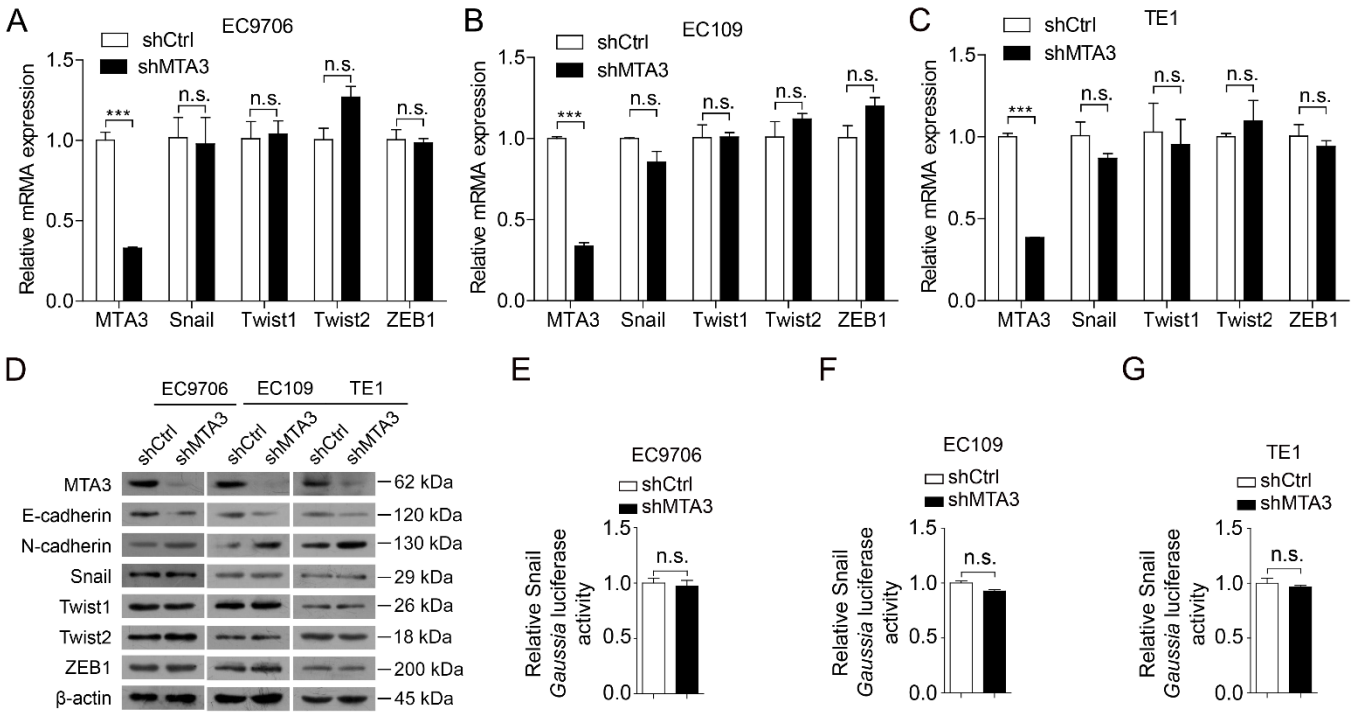

Figure S4. Related to Figure 2. MTA3 shows no effect on canonical EMT regulators. (**A-C**) QRT-PCR of *MTA3*, *Snai1*, *Twist1*, *Twist2* and *ZEB1* in EC9706 (A), EC109 (B) and TE1 (C) cells with MTA3 depleted. (**D**) Western blot of the indicated epithelial and mesenchymal markers, or EMT regulators in the indicated cells. (**E-G**) Snai1 luciferase reporter activity was analyzed in EC9706 (E), EC109 (F) and TE1 (G) cells with MTA3 depleted. Data were shown as the means from at least three independent experiments or representative data. Error bars indicate SEM. n.s., not statistically significant; ***p<0.001 by Student's *t*-test.

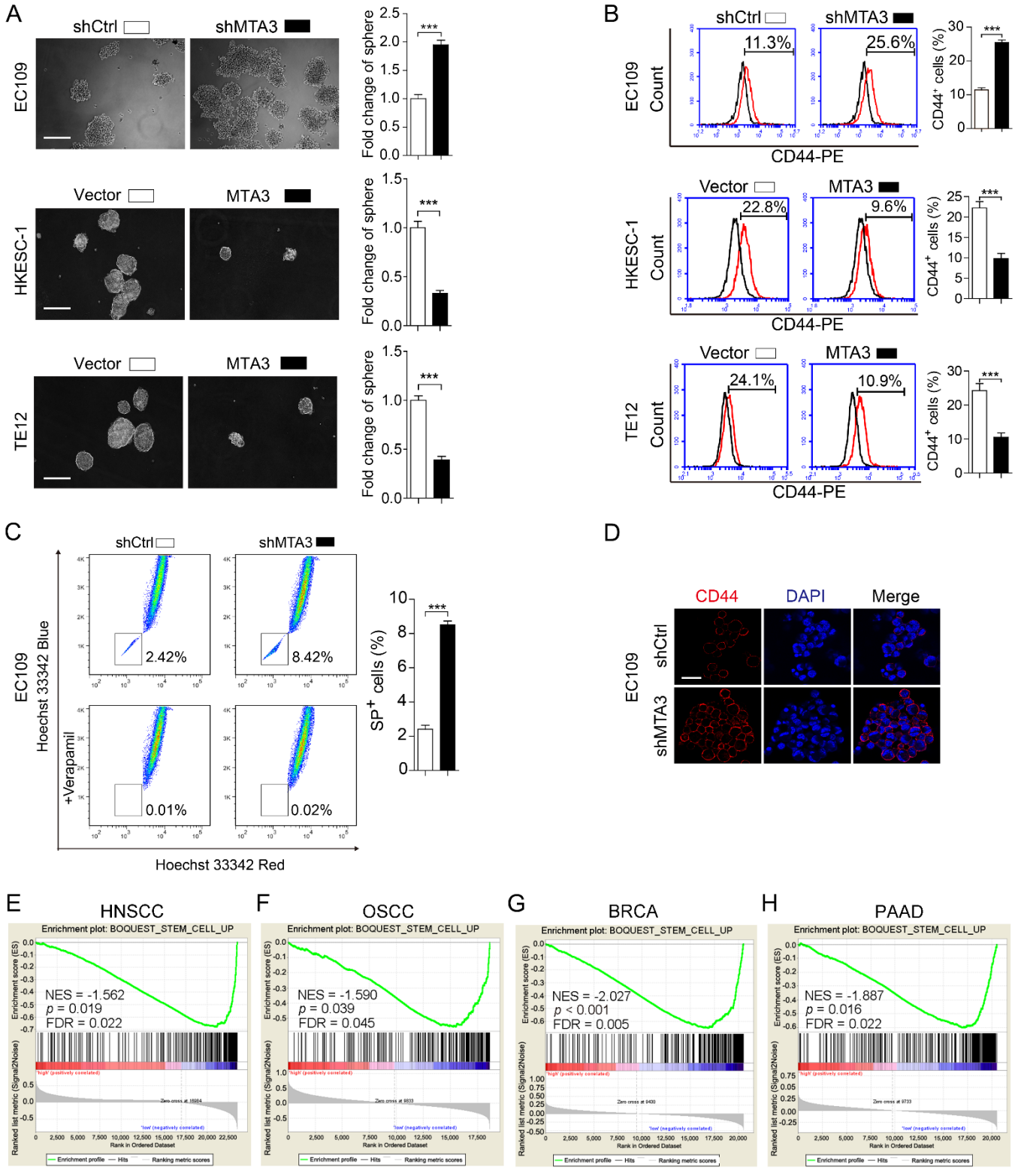

Figure S5. Related to Figure 2. MTA3 regulates stemness in ESCC cells and negatively correlates with stemness signature in various cancers. (**A**) Representative images of spheres formed by EC109 cells with MTA3 depleted, or HKESC-1 cells and TE12 cells with MTA3 overexpressed (left panel). Histograms showing the fold change in the number of spheres formed by EC109 cells with MTA3 depleted (right panel). Scale bars: 200 μm. (**B**) Flow cytometry analysis of the $CD44^+$ population in EC109 cells with MTA3

depleted, or HKESC-1 cells and TE12 cells with MTA3 overexpressed. Histograms showing the proportion of $CD44^+$ cells in the indicated cells (right panel). (**C**) Hoechst 33342 dye exclusion assay of the SP^+ population in EC109 cells with MTA3 depleted. Histograms showing the proportion of SP^+ cells in EC109 cells with MTA3 depleted (right panel) (**D**) Representative images of immunofluorescence for CD44 expression in EC109 cells with MTA3 depleted. Scale bars: 40 μm. (**E-H**) GSEA plots of enrichment of BOQOEST_STEM_CELL_UP signatures in $MTA3^{High}$ tumors versus $MTA3^{Low}$ tumors in the HNSCC (GEO dataset GSE10300, n = 44), OSCC (GEO dataset GSE37991, n = 40), BRCA (TCGA dataset, n = 1222), PAAD (TCGA dataset, n = 182). Data were shown as the means from at least three independent experiments or representative data. Error bars indicate SEM. ***$p<0.001$ by Student's *t*-test.

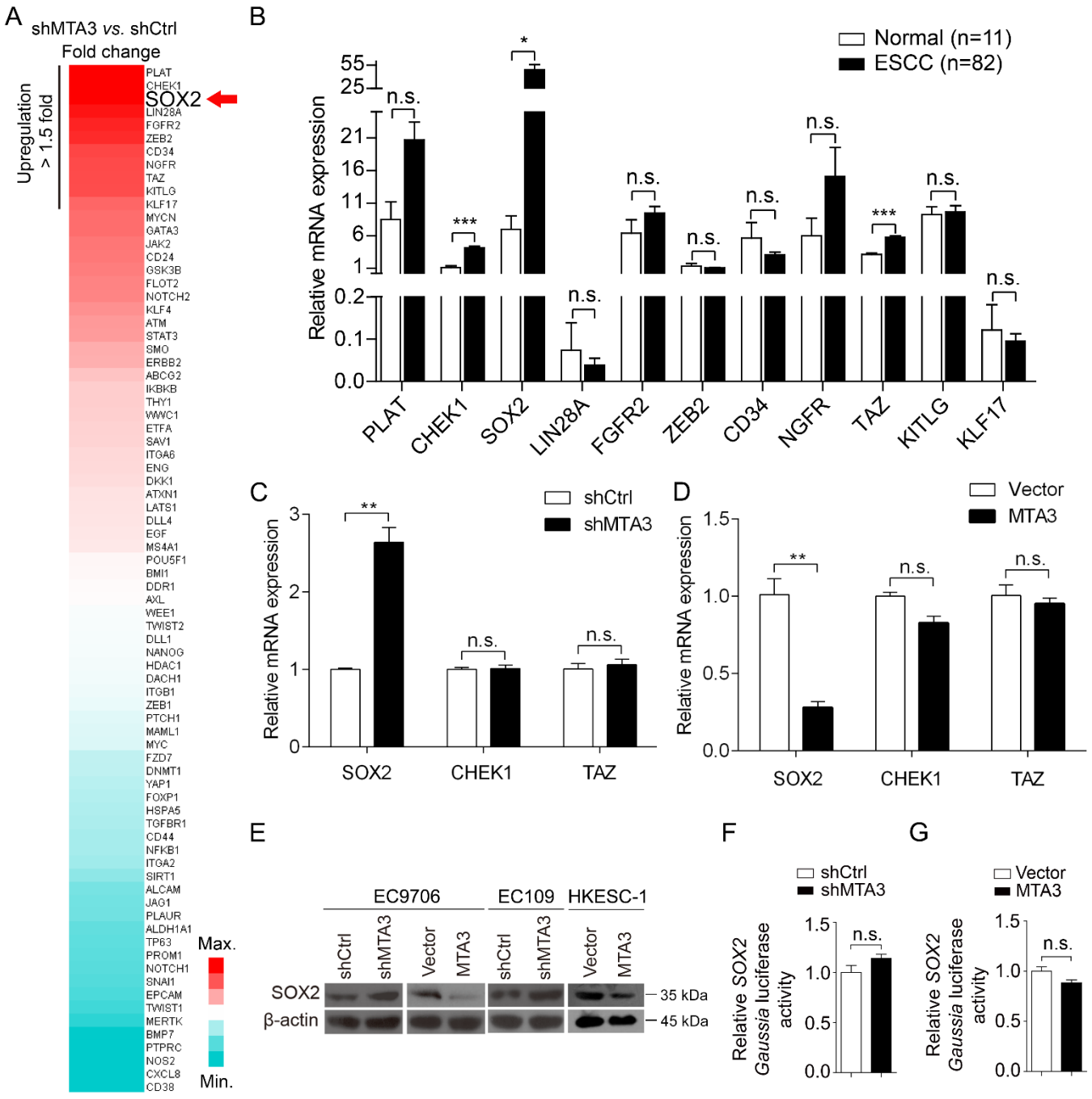

Figure S6. Related to Figure 3. MTA3 suppresses SOX2 expression indirectly. (**A**) Heat map showing fold change expression of stemness signatures in shMTA3 versus shCtrl EC9706 cells based on qPCR array. (**B**) The expression of 11 genes upregulated by MTA3 depletion (more than 1.5 folds) was analyzed in ESCC using TCGA dataset (Titled ESCA), which includes 82 ESCC tissues and 11 normal esophageal tissues. (**C** and **D**) QRT-PCR of SOX2, CHEK1, and TAZ in the indicated cells with MTA3 depleted (C) or overexpressed (D). (**E**) Western blot of SOX2 in EC9706 cells with MTA3 depleted or overexpressed and EC109 cells with MTA3 depleted, and HKECS-1 with MTA3 overexpressed. (**F and G**) SOX2 luciferase

reporter was transfected into EC9706 cells with MTA3 depleted (F) or overexpressed (G). The relative SOX2 Gaussia luciferase reporter activities were measured at 72 h after transfection. Data were shown as the means from at least three independent experiments or representative data. Error bars indicate Error bars indicate SEM. n.s., not statistically significant, *p<0.05, **p<0.01, **p<0.01 by Student's t-test.

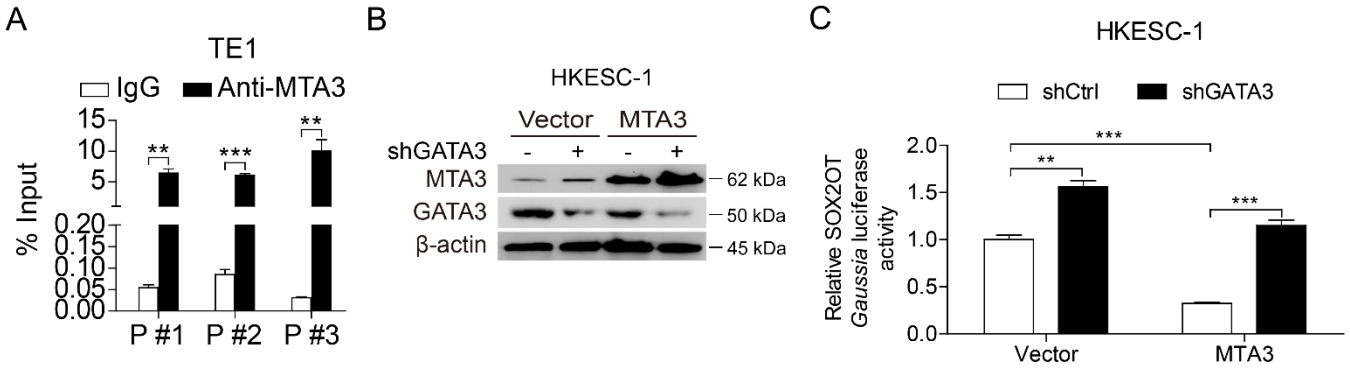

Figure S7. Related to Figure 3. MTA3-repressed SOX2OT transcription depends on GATA3. (**A**) ChIP assay using antibodies against MTA3 or IgG. qPCR to detect the enriched DNA fragments in the SOX2OT promoter region in TE1 cells. (**B**) Western blot of GATA3 in HKESC-1 transfected with the MTA3 or shGATA3 plasmids or in combinations between MTA3 and shGATA3. β-actin is shown as a loading control. (**C**) SOX2OT luciferase reporter activity in MTA3 overexpressed HKESC-1 cells that transfected with shGATA3 expressing plasmid. Data were shown as the means of three independent experiments or representative data. Error bars indicate SEM. $^{**}p < 0.01$, $^{***}p < 0.001$ by Student's *t*-test or a one-way ANOVA with post hoc intergroup comparisons, where appropriate.

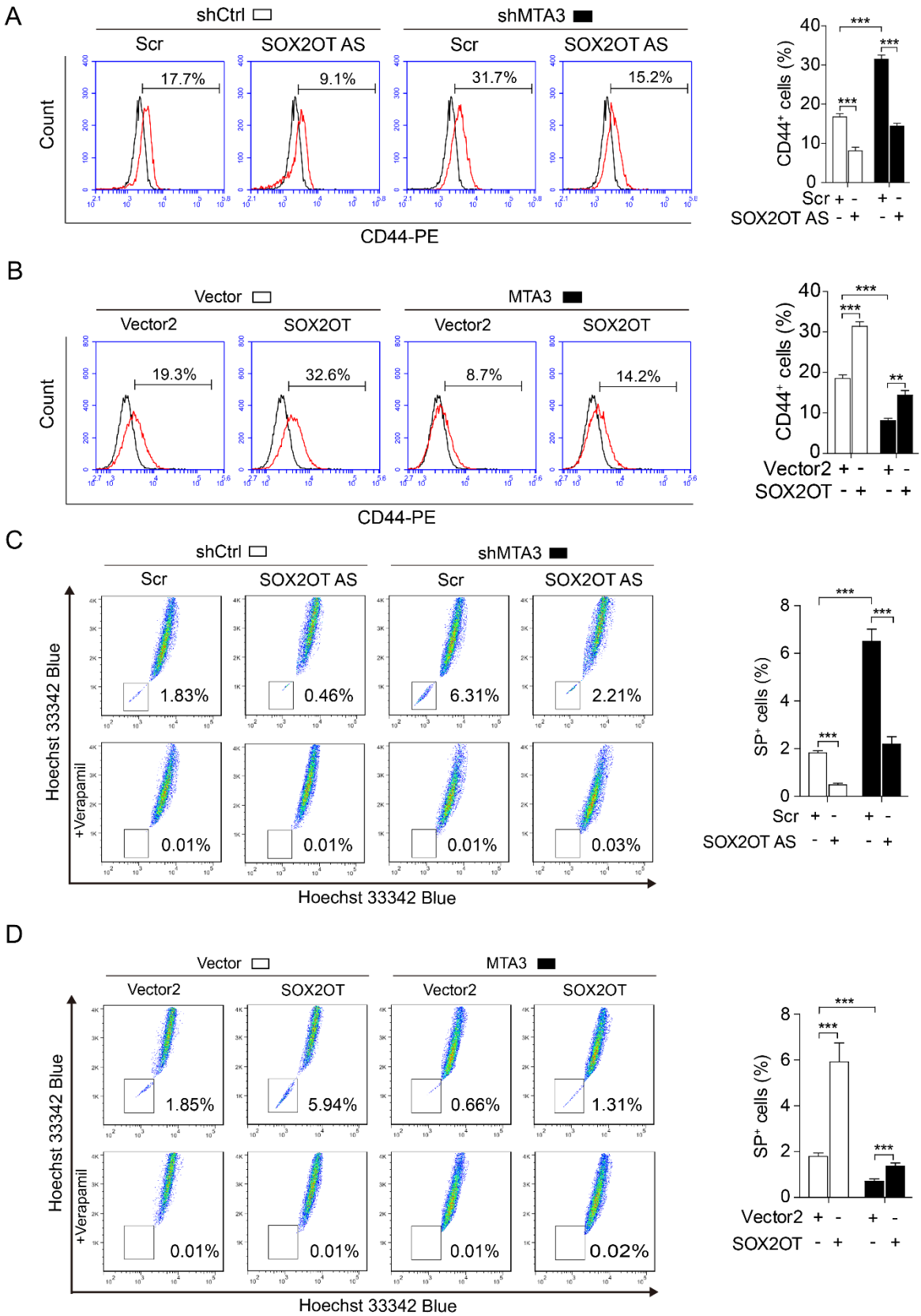

Figure S8. Related to Figure 4. MTA3 regulates CD44⁺ population and SP⁺ population via SOX2OT.

(**A** and **B**) EC9706 cells transfected with a combination of the shMTA3 expressing plasmid and SOX2OT AS oligo (A), or of the MTA3 and SOX2OT expressing plasmid (B) were subjected to flow cytometry

analysis of the $CD44^+$ population. (**C** and **D**) EC9706 cells transfected with a combination of the shMTA3 expressing plasmid and SOX2OT AS oligo (C), or of the MTA3 and SOX2OT expressing plasmid (D) were subjected to Hoechst 33342 dye exclusion assay of the SP^+ population. Histograms showing the positive formed by the indicated cells (right panels). Data were shown as the means from at least three independent experiments or representative data. Error bars indicate SEM. ***$p< 0.001$ by one-way ANOVA with post hoc intergroup comparisons.

Supplemental tables

Table S1. Related to Figure 1. Relationship between MTA3 expression and clinicopathologic variables in tissue samples of ESCC

Variables	No. of patients	MTA3 expression		*p*-value
		Low, no. (%)	High, no. (%)	
All patients	125	78 (62.4)	47 (37.6)	
Gender				
Male	93	58 (62.4)	35 (37.6)	0.989
Female	32	20 (62.5)	12 (37.5)	
Age (years)				
< 60	63	42 (66.7)	21(33.3)	0.321
≥ 60	62	36(58.1)	26 (61.9)	
Histologic grade				
Well	46	28 (60.9)	18 (39.1)	0.112
Moderate	64	37 (57.8)	27 (42.2)	
Poor	15	13 (86.7)	2 (13.3)	
Tumor size				
< 5 cm	46	31 (67.4)	15 (32.6)	0.379
≥ 5 cm	79	47 (59.5)	32 (40.5)	
Tumor depth				
T_1/T_2	23	9(39.1)	14 (60.9)	0.011
T_3/T_4	102	69 (67.6)	33 (32.4)	
Lymph node metastasis				
Negative	55	35(63.6)	20 (36.4)	0.800
Positive	70	43(61.4)	27 (38.6)	
Stage				
I-II	39	19(48.7)	20 (51.3)	0.033
III	86	59(68.6)	27 (31.4)	

[a.] ESCC, esophageal squamous cell carcinoma.

Table S2. Related to Figure 1. Univariate and multivariate Cox proportional hazards model predicting survival in ESCC

Variables	Univariate analysis HR (95% CI)	*p*-value	Multivariate analysis HR (95% CI)	*p*-value
Gender				
Male vs. Female	1.421(0.730-2.766)	0.301	1.787 (0.901-3.544)	0.097
Age				
≥ 60 *vs*. <60	1.526 (0.880-2.645)	0.132	1.712 (0.973-3.014)	0.062
Histologic grade				
Poor / Moderate *vs*. Well	1.586 (0.879-2.860)	0.126	1.663 (0.855-3.235)	0.134
Tumor size				
≥ 5 cm *vs*. < 5 cm	1.237 (0.698-2.191)	0.466	1.062 (0.586-1.922)	0.844
Tumor depth				
T_3/T_4 *vs*. T_1/T_2	3.332 (1.200-9.246)	0.021	1.487 (0.494-4.472)	0.480
Lymph node metastasis				
Positive *vs*. Negative	1.484 (0.844-2.612)	0.170	0.911 (0.465-1.783)	0.786
Stage				
III *vs*. I/II	3.940 (1.774-8.750)	0.001	3.417 (1.360-8.586)	0.009
MTA3 expression				
Low *vs*. High	2.988 (1.498-5.958)	0.002	2.717 (1.333-5.537)	0.006

[a.] ESCC, esophageal squamous cell carcinoma; [b.] HR, hazard ratio; [c.]CI, confidence interval.

Table S3. Related to Figure 3. Summary of GATA3 genetic change in ESCC

Study cohorts	Mutation	Amplification	Deletion	Total
Esophageal Carcinoma (TCGA, Provisional)	0	1	1	96
Esophageal Squamous Cell Carcinoma (UCLA, Nat Genet 2014)	0	0	0	139
Esophageal Squamous Cell Carcinoma (ICGC, Nature 2014)	0	0	0	88
Total	0	1	1	323

[a.] ESCC, esophageal squamous cell carcinoma; [b.] TCGA, the Cancer Genome Atlas; [c.] UCLA, University of California, Los Angeles; [d.] ICGC, International Cancer Genomics Consortium.

Transparent Methods

Clinical patients and samples

Paraffin-embedded specimens and snap-frozen fresh ESCC tissues with their normal adjacent tissues were obtained from ESCC patients underwent surgeries at Affiliated Tumor Hospital of Shantou University Medical College. All samples were histopathologically and clinically diagnosed as ESCC. Patients who underwent preoperative neoadjuvant chemotherapy or radiotherapy for ESCC were excluded from this study.

Tissue microarray and immunohistochemistry

A tissue microarray (TMA) was conducted using paraffin-embedded specimens from 125 ESCC patients (male, n = 93; Female, n = 32) and their normal adjacent tissues as previously described (Dong et al., 2017b). Immunohistochemistry (IHC) staining was performed as previously described (Dong et al., 2017b). Briefly, the TMA blocks or the tumor xenograft tissues were sliced into 4-μm sections and immune-stained with antibodies against MTA3 (Bethyl Laboratories Inc., catalog no. A300-160A), SOX2 (Cell Signaling Technology, catalog no. 23064), or CD44 (Cell Signaling Technology, catalog no. 3570). Immunostaining scores were determined by combination of staining intensity and the percentage of positively stained cells. Staining intensity was categorized as follows: 1, negative; 2, light yellow; 3, brown. The proportion of positive cells was scored as follows: 0 (0% positive cells); 1 (1%–25% positive cells); 2 (26%–50% positive cells); 3 (51%–75% positive cells); 4 (76%–100% positive cells). Two independent pathologists without the clinical and pathological information independently reviewed and scored the immunostaining.

Cell lines and cell culture

The human ESCC cell lines EC109 and EC9706 (obtained from the Cell Bank of the Chinese Academy of

Sciences, Shanghai, China), and HKESC-1, HKESC-2, and HKESC-3 (kindly provided by Dr. S.W. Tsao, University of Hong Kong, China), and KYSE510 (obtained from the American Type Culture Collection) were cultured in RPMI 1640 (Gibco/Invitrogen) supplemented with 10% FBS (Gibco/Invitrogen). TE1 and TE12 (kindly provided by Dr. X.C. Xu, UT M.D. Anderson Cancer Center, USA) were cultured in Dulbecco's Modified Eagle Media (DMEM, Gibco/Invitrogen) supplemented with 10% FBS (Gibco/Invitrogen). The human immortalized esophageal epithelial cell lines NE2 and NE3 (kindly provided by Dr. S.W. Tsao, University of Hong Kong, China) were cultured in Defined Keratinocyte-SFM medium (DK-SFM, Gibco/Invitrogen). EC109, EC9706, HKEC-1, HKESC-3, TE1 and TE12 were derived from male patients with ESCC. HKESC-2 and KYSE-510 were derived from female patients with ESCC. NE2 and NE3 were derived from normal human esophageal tissue samples.

Transfection and infection

The full-length cDNA of MTA3 was PCR amplified from EC9706 cells and cloned into the pCDNA3.1-flag plasmid. The shRNA targeting human MTA3 (target sequence: GAGGATACCTTCTTCTACTCA) was cloned into pBabe/U6 plasmid. The plasmid carrying SOX2, and the plasmid carrying shGATA3 or shSOX2 targeted to the human GATA3 or SOX2 (shGATA3 target sequence: GATGCAAGTCCAGGCCCAA; shSOX2 target sequence: GGTTGACACCGTTGGTAATTT) were obtained from GeneCopoeia. The pEZX-PG04 plasmid carrying double-expression cassette for *Gaussia* luciferase (GLuc) under the control of the SOX2OT, SOX2, or Snai1 promoter, and secreted Alkaline Phosphatase (SeAP) under the control of CMV promoter were obtained from GeneCopoeia. pIRES2-ZsGreen1-SOX2OT plasmid and SOX2OT-GLuc plasmid with deletion of GATA3 binding sites between −1176 to −1169 bp (ΔGATA3 #1), −861 to −854 bp (ΔGATA3 #2), −291 to −284 bp (ΔGATA3 #3), or all the three GATA3 binding sites were constructed by Youbio (Hunan, China). The antisense locked nucleic acid (LNA) GapmeR targeting SOX2OT (SOX2OT AS): 5'-TCTTACTGAATGGAGG-3' and non-targeting LNA GapmeR (Scr): 5'-

AACACGTCTATACGC-3’ were obtained from Exiqon (Vedbaek, Denmark). Recombinant lentiviruses carrying luciferase gene were obtained from GeneChem (Shanghai, China). Transfection of plasmids or LNA GapmeR was performed using Lipofectamine 3000 (Thermo Fisher Scientific, catalog no. L3000015) according to the manufacturer’s instructions. Concentrated viruses carrying luciferase gene were used to infect cells in a 6-well plate with 10 μg/ml polybrene.

The quantitative real-time PCR assay

Total RNA was isolated from cultured cells, ESCC tissues or xenograft tissues by the TRIzol reagent (ThermoFisher, catalog no. 15596-018), and reverse transcribed using High Capacity cDNA Reverse Transcription Kit (Applied Biosystems, catalog no. 4368813) according to the manufacturer instructions. The cDNA was amplified and quantified in the ABI-7500 system (Applied Biosystems) by using SYBR Green Master (Roche). The cDNA was subjected to quantitative real-time PCR (qRT-PCR) with the following primers: *MTA3* forward: 5’-AAGCCTGGTGCTGTGAAT-3’ and reverse: 5’-AGGGTCCTCTGTAGTTGG-3’; *SOX2OT* forward: 5’-GCTCGTGGCTTAGGAGATTG-3’ and reverse: 5’-CTGGCAAAGCATGAGGAACT-3’; *SOX2* forward: 5’-CATCACCCACAGCAAATGACA-3’ and reverse: 5’-GCTCCTACCGTACCACTAGAACTT-3’; *Snai1* forward: 5’-TCTGAGGCCAAGGATCTCCA-3’ and reverse: 5’-CATTCGGGAGAAGGTCCGAG-3’; *Twist1* forward: 5’-AGACCTAGATGTCATTGTTTCCA-3’ and reverse: 5’-TTGGCACGACCTCTTGAGAAT-3’; *Twist2* forward: 5’-CTGCCATTGCCAGACCTTCT-3’ and reverse: 5’-GATGGTGTTGGCAGTGTTGC-3’; *ZEB1* forward: 5’-TTCTCCCTCCCCTCTGGGAT-3’ and reverse: 5’-CCTATGCTCCACTCCTTGCT-3’; *Luciferase* forward: 5’-ACTGGGACGAAGACGAACAC-3’ and reverse: 5’-GGCGACGTAATCCACGATCT-3’; *β-actin* forward: 5’-GAACCCCAAGGCCAACCGCGAGA-3’ and reverse: 5’-TGACCCCGTCACCGGAGTCCATC-3’.

Western blot analysis

Proteins in the lysates of the cultured cells or xenograft tissues were separated on SDS-PAGE, transferred onto the PVDF membranes. The membranes were incubated with primary antibodies against MTA3 (Bethyl Laboratories Inc., catalog no. A300-160A), SOX2 (Cell Signaling Technology, catalog no. 23064), E-Cadherin (BD Bioscience, catalog no. 610181), N-Cadherin (BD Bioscience, catalog no. 610920), Vimentin (Cell Signaling Technology, catalog no. 3932), GATA3 (Santa Cruz Biotechnology, catalog no. sc-268), Snai1 (Cell Signaling Technology, catalog no. 3879), Twist1 (Cell Signaling Technologies, catalog no. 46702), Twist2 (Abcam, catalog no. ab66031), and ZEB1 (Abcam, catalog no. ab203829), and β-actin (Cell Signaling Technology, catalog no. 4970), followed by HRP-conjugated secondary antibodies as previously described (Feng et al., 2014). Protein bands were visualized with SuperSignal West Pico Luminol/Enhancer Solution (Thermo Scientific).

Transwell assay

After starvation for 24 h, the cells (1×10^5) in 200ul serum-free RPMI 1640 were seeded onto the upper compartment of a 24-well chamber pre-coated with (Invasion assay) or without (Migration assay) matrigel (BD Biosciences, catalog no. 356234). The lower compartment was filled with 500ul RPMI 1640 supplemented with 10% FBS. After 24-48 h of incubation, the invaded/migrated cells were fixed with methanol, stained with 0.1% crystal violet, and counted under a microscope. All experiments were performed in triplicate.

Phalloidin staining

Cells were fixed with 4% paraformaldehyde for 20 min and blocked in 5% BSA for 30 min at room temperature. Fixed cells were then incubated with 5μg/ml of phalloidin (Invitrogen, catalog no. A12381) in dark for 30 min at 37°C. Phalloidin staining was observed under ZEISS LSM800 confocal fluorescence microscope (ZEISS, Germany).

Sphere formation assays

Cells were seeded in 6-well ultra-low attachment plates (Corning, catalog no. 3471) in DMEM/F12 serum-free medium (Gibco/Invitrogen) supplemented with 10 ng/ml EGF (PeproTech, catalog no. AF-100-15), 10 ng/ml bFGF (PeproTech, catalog no. 100-18B) and 1×N2 (Life Technologies, catalog no. 17502-048). After incubation of 1-2 weeks, the number of tumorspheres was counted under a microscope (Olympus, Tokyo, Japan).

Flow cytometry

For $CD44^+$ subpopulation analysis, cells were suspended in 250μl ice-cold PBS and incubated with either anti-Human/Mouse CD44 PE-Cyanine5 antibody (eBioscience, catalog no. 15-0441) or Rat IgG2b K Isotype Control PE-Cyanine5 (eBioscience, catalog no. 15-4031) for 90 min at 4°C with gentle rotation. Then, the cells were washed twice with ice-cold 1×PBS before flow cytometric analysis. The data were analyzed by BD Accuri C6 Software (BD Biosciences, USA). For hoechstside-population analysis, cells were suspended in 500μl of DMEM supplemented with 10% FBS and pre-incubated with or without 100 μM verapamil (Sigma-Aldric, catalog no. V4629) for 15 min at 37°C. Subsequently, the cells were incubated with 5 μg/ml Hoechst 33342 dye (Sigma-Aldrich, catalog no. 14533) for 1 h at 37°C. Finally, the cells were incubated on ice for 5 min and washed twice with ice-cold 1×PBS before flow cytometric analysis. The data were analyzed by FlowJo 10 (FLOWJO, LLC, Ashland, USA).

Immunofluorescence and confocal microscopy assays

Spheres were collected by centrifugation at 1500×g for 5 min and gently resuspended in 1×PBS. The suspension was transferred to a glass slide and a smear was prepared. The smear was left to dry at 37°C followed by immunofluorescence analysis as described previously (Gan et al., 2016). Nuclei were stained with DAPI. Images were captured using ZEISS LSM800 confocal fluorescence microscope (ZEISS,

Germany).

Stemness signatures-related gene qPCR array

The cDNA of EC9706 cells transfected with shMTA3 or shCtrl was used for stemness signature analysis using Custom Gene qPCR Arrays (GeneCopoeia, catalog no. PAG-CS). The mRNA levels of 78 stemness genes were measured by SYBR™ Green PCR Master Mix (Applied Biosystems, catalog no. 4309155) with the Applied Biosystems 7500 Real-Time PCR system (Applied Biosystems).

Gaussia luciferase assay

Cells were transiently transfected with the indicated *Gaussia* luciferase plasmids using Lipofectamine 3000 (Thermo Fisher Scientific, catalog no. L3000015) according to the manufacturer's instructions, and incubated for 72 hours. The culture medium was collected and subjected for analysis of *Gaussia* luciferase (GLuc) and secreted Alkaline Phosphatase (SeAP) activities using a Secrete-PairTM Dual Luminescence Assay Kit (GeneCopoeia, catalog no. SPDA-D010) according to the manufacturer's instructions. GLuc activity was normalized to SeAP activity.

Chromatin immunoprecipitation assay

The chromatin immunoprecipitation (ChIP) assay was performed using an EZ-Magna ChIP™ A ChIP kit (Millipore, catalog no. 17-408) as described previously (Dong et al., 2017b). Briefly, cells were cross-linked with 1% (v/v) formaldehyde on ice for 10 minutes and sonicated to shear chromatin DNA into ~200-1000 bp in length by a Bioruptor Sonicator (Diagenode, Sparta, NJ, USA). Immunoprecipitation was done with antibodies against MTA3 (Bethyl Laboratories Inc., catalog no. A300-160A) or IgG (Sigma Aldrich, St Louis, MO, USA) with 20μl of protein A magnetic beads gently rotated at 4°C overnight. After washing by wash buffer, the immunoprecipitated DNA was then used for semi-quantitative PCR or qPCR analysis using

the following primers: P #1 forward: 5’-AGAGAATCTCAAGGTCACCAGG-3’ and reverse: 5’-TGGCCATTCTTTTGCACTTGG-3’; P #2 forward: 5’-CATGCAATTTACTCTGGAGGCA-3’ and reverse: 5’-TTCATCACTTCTGCAATTGACCA-3’; P #3 forward: 5’-AATTGTGAACACTGTTTTTAAGCAA-3’ and reverse: 5’-CCCTAAGTGTGCCATTTGCC-3’; GADPH (negative control) forward: 5'-TCCTCCTGTTTCATCCAAGC-3' and reverse: 5'-TAGTAGCCGGGCCCTACTTT-3' (Si et al., 2015). 1% of the supernatant was used as input.

Proximity ligation assay

The Proximity Ligation Assay (PLA) kit (Duolink®using PLA®Technology, Sigma–Aldrich) was employed to detect the interaction between MTA3 and GATA3 (Dong et al., 2017a). In brief, cells grown on glass coverslips were fixed with 4% paraformaldehyde followed by permeabilization in 0.2% Triton X-100 and blocking in 5% BSA. The cells were then incubated with rabbit anti-MTA3 and mouse anti-GATA3 antibodies and followed by incubation with secondary plus and minus probes, PLA–anti-(rabbit IgG) and PLA–anti-(mouse IgG). The ligation solution was added followed by an amplification solution. The PLA signals were visualized under ZEISS LSM800 confocal fluorescence microscope (ZEISS, Germany).

Animal experiments

For tumor growth assay, xenografting was performed as described previously (Dong et al., 2017b). Briefly, indicated cells (1×10^6 cells for EC9706 and EC109; 4×10^6 cells for HKESC-1) were injected subcutaneously into flanks of 5- to 6-week-old female nude mice (Vital River Laboratory Animal Technology Co. Ltd.). The tumor growth was monitored for 4 or 5 weeks. The tumor size was measured weekly using a slide caliper and tumor volume was calculated by the following formula: volume = 0.5236 × length × width^2. At the end of the experiment, mice were sacrificed and tumors were excised, photographed and used for RNA and protein purification or reserved in paraffin block. For inguinal lymph

node metastasis, cells were infected with recombinant lentiviruses carrying luciferase, and these cells (1×10^6 cells for EC9706; 5×10^6 cells for TE1) were injected subcutaneously into the flanks of 5- to 6-week-old female nude mice (8 mice per group). The mice were monitored for inguinal lymph node metastasis once weekly by injection of 150 mg/kg of D-luciferin (Solarbio, Beijing, China; catalog no. D9390) intraperitoneally. 10-15 min after injection, mice were anesthetized and bioluminescence was imaged with Xenogen IVIS System (Xenogen). Mice were sacrificed at day 32, 15 min before mice were sacrificed, D-luciferin was injected intraperitoneally. After sacrificing, the inguinal lymph nodes were harvested and analyzed for the presence of metastatic cells using Xenogen IVIS System (Xenogen). The inguinal lymph nodes were then subjected for paraffin blocks, and then tissue sections were stained with H&E for histological validation. For lung metastasis, 1×10^6 of cells were injected into the tail vein of 5- to 6-week-old female nude mice (6 mice per group). Mice were sacrificed at day 61 and the lungs were fixed in Bouins for 24 hours. The lungs were photographed, paraffin blocked, and sectioned for staining.

Bioinformatic analysis

The protein levels of MTA3 in different organs were obtained from the Human Protein Atlas database (https://www.proteinatlas.org) (Uhlen et al., 2015).ESCC datasets GSE23400 (Su et al., 2011) and GSE26886 (Wang et al., 2013) were obtained from the NCBI Gene Expression Omnibus (GEO. https://www.ncbi.nlm.nih.gov/geo/) (Barrett et al., 2007) to detect the levels of MTA3. The level of MTA3 mRNA in ESCC cell lines was analyzed in dataset GSE23964 from GEO. A TCGA dataset (Titled ESCA), which includes 81 ESCC tissues and 11 normal esophageal tissues, was downloaded from the TCGA database (https://cancergenome.nih.gov/) and analyzed. The alteration of *GATA3* gene in ESCC was analyzed using cBioPortal database (https://www.cbioportal.org/) (Gao et al., 2013).

Gene Set Enrichment Analysis

The ESCC dataset GSE23400 (Su et al., 2011) and GSE47404 (Sawada et al., 2015), head and neck squamous cell carcinoma (HNSCC) dataset GSE10300 (Cohen et al., 2009), oral squamous cell carcinoma (OSCC) dataset GSE37991 (Lee et al., 2013) from GEO, and Breast invasive carcinoma (BRCA) dataset, Pancreatic adenocarcinoma (PAAD) dataset from TCGA database were analyzed using GSEA software (Version 2.2.1, http://software.broadinstitute.org/gsea/index.jsp) as previously described (Dong et al., 2017a; Dong et al., 2017b).

Statistics

All data were analyzed using the SPSS 17.0 software (SPSS Inc., USA). Receiver operating characteristic (ROC) curve analysis was performed to define the cutoff score for the expression of MTA3 and SOX2. The $\chi 2$ test was used to analyze the correlation between the expression of MTA3 and clinicopathological parameters of ESCC patients, the difference between the proportion of inguinal lymph nodes metastasis or lung metastasis in shMTA3 and shCtrl mice. Kaplan–Meier was used in plotting the survival curves, and the difference was compared by log-rank test. Univariate and multivariate Cox regression survival analyses were done to evaluate the survival data. Student's *t*-test was used to compare the difference between two groups, and one-way ANOVA with post hoc intergroup comparisons was performed to compare the difference among more than two groups. Pearson's correlation coefficients were performed to determine the correlations of the mRNA expression between *MTA3* and the indicated genes in ESCC tissues. All data were presented as the mean ± SEM. A p-value < 0.05 was considered statistically significant.

Study approval

Clinical research protocols of this study were reviewed and approved by the Ethics Committee of Cancer Hospital of Shantou University Medical College (IRB serial number: #04-070). Written informed consent was obtained from patients in accordance with principles expressed in the Declaration of Helsinki. Animals

were housed in conventional or pathogen-free conditions, where appropriate, at the Animal Center of Shantou University Medical College, in compliance with Institutional Animal Care and Use Committee (IACUC) regulations (SUMC2014-148). All animal experiments were performed according to protocols approved by the Animal Care and Use Committee of the Medical College of Shantou University.

Supplemental References

Barrett, T., Troup, D.B., Wilhite, S.E., Ledoux, P., Rudnev, D., Evangelista, C., Kim, I.F., Soboleva, A., Tomashevsky, M., and Edgar, R. (2007). NCBI GEO: mining tens of millions of expression profiles--database and tools update. Nucleic Acids Res *35*, D760-765.

Cohen, E.E., Zhu, H., Lingen, M.W., Martin, L.E., Kuo, W.L., Choi, E.A., Kocherginsky, M., Parker, J.S., Chung, C.H., and Rosner, M.R. (2009). A feed-forward loop involving protein kinase Calpha and microRNAs regulates tumor cell cycle. Cancer Res *69*, 65-74.

Dong, H., Ma, L., Gan, J., Lin, W., Chen, C., Yao, Z., Du, L., Zheng, L., Ke, C., Huang, X., et al. (2017a). PTPRO represses ERBB2-driven breast oncogenesis by dephosphorylation and endosomal internalization of ERBB2. Oncogene *36*, 410-422.

Dong, H., Xu, J., Li, W., Gan, J., Lin, W., Ke, J., Jiang, J., Du, L., Chen, Y., Zhong, X., et al. (2017b). Reciprocal androgen receptor/interleukin-6 crosstalk drives oesophageal carcinoma progression and contributes to patient prognosis. J Pathol *241*, 448-462.

Feng, Y., Ke, C., Tang, Q., Dong, H., Zheng, X., Lin, W., Ke, J., Huang, J., Yeung, S.C., and Zhang, H. (2014). Metformin promotes autophagy and apoptosis in esophageal squamous cell carcinoma by downregulating Stat3 signaling. Cell Death Dis *5*, e1088.

Gan, J., Ke, X., Jiang, J., Dong, H., Yao, Z., Lin, Y., Lin, W., Wu, X., Yan, S., Zhuang, Y., et al. (2016). Growth hormone-releasing hormone receptor antagonists inhibit human gastric cancer through downregulation of PAK1-STAT3/NF-kappaB signaling. Proc Natl Acad Sci U S A *113*, 14745-14750.

Gao, J., Aksoy, B.A., Dogrusoz, U., Dresdner, G., Gross, B., Sumer, S.O., Sun, Y., Jacobsen, A., Sinha, R., Larsson, E., et al. (2013). Integrative analysis of complex cancer genomics and clinical profiles using the cBioPortal. Sci Signal *6*, pl1.

Lee, C.H., Wong, T.S., Chan, J.Y., Lu, S.C., Lin, P., Cheng, A.J., Chen, Y.J., Chang, J.S., Hsiao, S.H., Leu, Y.W., et al. (2013). Epigenetic regulation of the X-linked tumour suppressors BEX1 and LDOC1 in oral squamous cell carcinoma. J Pathol *230*, 298-309.

Sawada, G., Niida, A., Hirata, H., Komatsu, H., Uchi, R., Shimamura, T., Takahashi, Y., Kurashige, J., Matsumura, T., Ueo, H., et al. (2015). An Integrative Analysis to Identify Driver Genes in Esophageal Squamous Cell Carcinoma. PLoS One *10*, e0139808.

Si, W., Huang, W., Zheng, Y., Yang, Y., Liu, X., Shan, L., Zhou, X., Wang, Y., Su, D., Gao, J., et al. (2015). Dysfunction of the Reciprocal Feedback Loop between GATA3- and ZEB2-Nucleated Repression Programs Contributes to Breast Cancer Metastasis. Cancer Cell *27*, 822-836.

Su, H., Hu, N., Yang, H.H., Wang, C., Takikita, M., Wang, Q.H., Giffen, C., Clifford, R., Hewitt, S.M., Shou, J.Z., et al. (2011). Global gene expression profiling and validation in esophageal squamous cell carcinoma and its association with clinical phenotypes. Clin Cancer Res *17*, 2955-2966.

Uhlen, M., Fagerberg, L., Hallstrom, B.M., Lindskog, C., Oksvold, P., Mardinoglu, A., Sivertsson, A., Kampf, C., Sjostedt, E., Asplund, A., et al. (2015). Proteomics. Tissue-based map of the human proteome. Science *347*, 1260419.

Wang, Q., Ma, C., and Kemmner, W. (2013). Wdr66 is a novel marker for risk stratification and involved in epithelial-mesenchymal transition of esophageal squamous cell carcinoma. BMC Cancer *13*, 137.